Journal of Alloys and Compounds 515 (2012) 39–43

Contents lists available at SciVerse ScienceDirect

Journal of Alloys and Compounds

journal homepage: www.elsevier.com/locate/jallcom

Blue emission of $Sr_{2-x}Ca_xP_2O_7:Eu^{2+}$ for near UV excitation

Jinying Yu[a,b], Xia Zhang[a,*], Zhendong Hao[a], Yongshi Luo[a], XiaoJun Wang[c], Jiahua Zhang[a,*]

[a] Key Laboratory of Excited State Processes, Changchun Institute of Optics, Fine Mechanics and Physics, Chinese Academy of Sciences, Changchun 130033, China
[b] Graduate School of Chinese Academy of Sciences, Beijing 100039, China
[c] Department of Physics, Georgia Southern University, Statesboro, GA 30460, USA

ARTICLE INFO

Article history:
Received 2 September 2011
Received in revised form 12 October 2011
Accepted 13 October 2011
Available online 15 November 2011

Keywords:
Photoluminescence
Structure
Phosphor

ABSTRACT

$Sr_{2-x}Ca_xP_2O_7:Eu^{2+}$ ($x = 0-2$) phosphors with intense and adjustable blue emission are prepared by solid state reaction. The crystal phase evolution and correlated photoluminescence properties are studied as a function of Ca^{2+} content based on the experimental measurements of X-ray diffraction, photoluminescence and fluorescence decay. Our results indicate that $Sr_{2-x}Ca_xP_2O_7:Eu^{2+}$ crystallize in single α-$Sr_2P_2O_7$ type phase for $x \leq 0.75$. As increasing x from 0.75, α-$Ca_2P_2O_7$ type phase starts to form and increase followed by reduction of α-$Sr_2P_2O_7$ type phase. The single α-$Ca_2P_2O_7$ type phase is obtained only at $x = 2$. The emission band (band I) in α-$Sr_2P_2O_7$ type phase and that (band II) in α-$Ca_2P_2O_7$ type phase both shift to the red on increasing x due to enhancement of crystal field strength in case of Ca^{2+} substitution for Sr^{2+}. This substitution also leads to remarkably inhomogeneous broadening of band I, within which energy transfer from the high energy Eu^{2+} to the low energy one is observed. The superposition of band I and band II results in various distributions of intense emission band including the redshifted and more broadened ones suitable for white light generation.

1. Introduction

Eu^{2+} activated highly efficient blue emitting pyrophosphate phosphors $Sr_2P_2O_7:Eu^{2+}$ and $Ca_2P_2O_7:Eu^{2+}$ were studied in the early 1970s for application to the fluorescent lamp lighting [1]. Since the development of GaN based blue and near ultraviolet (UV) light emitting diodes (LEDs) at the end of last century, the solid state lighting sources based on white LEDs fabricated using blue (~460 nm) and/or near UV (~400 nm) LED chips coated with phosphors have been widely studied [2–8]. The white LEDs employing near UV LED chips with tricolor phosphors have the advantage of less shift of color point against forward current because the white light is completely phosphor converted not like the combination of blue LED with the yellow emitting YAG:Ce^{3+} phosphor [2]. Upon near UV excitation, α-$Sr_2P_2O_7:Eu^{2+}$ and α-$Ca_2P_2O_7:Eu^{2+}$ strongly emit at 420 nm and 416 nm, respectively [9,10]. Our previous study demonstrated that α-$Ca_2P_2O_7:Eu^{2+}$ allows Mn^{2+} to incorporate into its matrix to generate a strong additional band in orange originated from Mn^{2+} through Eu^{2+}–Mn^{2+} energy transfer, resulting in dual color (blue and orange) emissions for near UV LED chip based white LEDs [10]. However, both α-$Sr_2P_2O_7:Eu^{2+}$ and α-$Ca_2P_2O_7:Eu^{2+}$ emit at short wavelength of blue with bandwidth merely around 20 nm. To generate ideal white light, to broaden and shift the blue band to longer wavelength is expected.

The present paper demonstrates adjustable emission position and bandwidth of Eu^{2+} in $Sr_{2-x}Ca_xP_2O_7$. The crystal phase evolution and correlated photoluminescence properties are systematically studied as a function of Ca^{2+} content based on the experimental measurements of X-ray diffraction, photoluminescence and fluorescence decay. The redshifted and broadened blue emission band is achieved.

2. Experimental

The $Sr_{2-x}Ca_xP_2O_7:Eu^{2+}$ phosphors have been prepared by conventional solid-state reaction. The starting materials, analytical grade, $SrHPO_4$, $CaHPO_4$, $(NH_4)_2HPO_4$ and Eu_2O_3 were employed in molar ratio of $Sr_{2-x}Ca_xP_2O_7$:4% Eu^{2+} with various x ($x = 0$, 0.25, 0.5, 0.75, 1, 1.25, 1.5, 1.75, 2). After a good mixing in an agate mortar, the mixtures were sintered at 1200 °C for 4 h under a CO reducing atmosphere. All the experiments were performed at room temperature. The structure of sintered samples was identified by X-ray powder diffractometer (XRD) (Rigaku D/M AX-2500V). The measurements of photoluminescence (PL) and photoluminescence excitation (PLE) spectra were performed by a Hitachi F4500 fluorescent spectrometer. In fluorescence lifetime measurements, the third harmonic (355 nm) of a Nd doped yttrium aluminum garnet laser (Spectra-Physics, GCR130) was used as an excitation source, and the signals were detected with a Tektronix digital oscilloscope (TDS 3052).

3. Results and discussion

Fig. 1(a) shows the XRD patterns of $Sr_{2-x}Ca_xP_2O_7$:4% Eu^{2+} ($x = 0$, 0.25, 0.5, 0.75, 1, 1.25, 1.5, 1.75, 2) phosphors in the 2θ range of 20–50°. One can observe the evolution of crystalline structure from

* Corresponding author. Tel.: +86043186708875; fax: +86043186708875.
E-mail addresses: xzhang31@yahoo.cn (X. Zhang), zhangjh@ciomp.ac.cn (J. Zhang).

0925-8388/$ – see front matter © 2011 Published by Elsevier B.V.
doi:10.1016/j.jallcom.2011.10.043

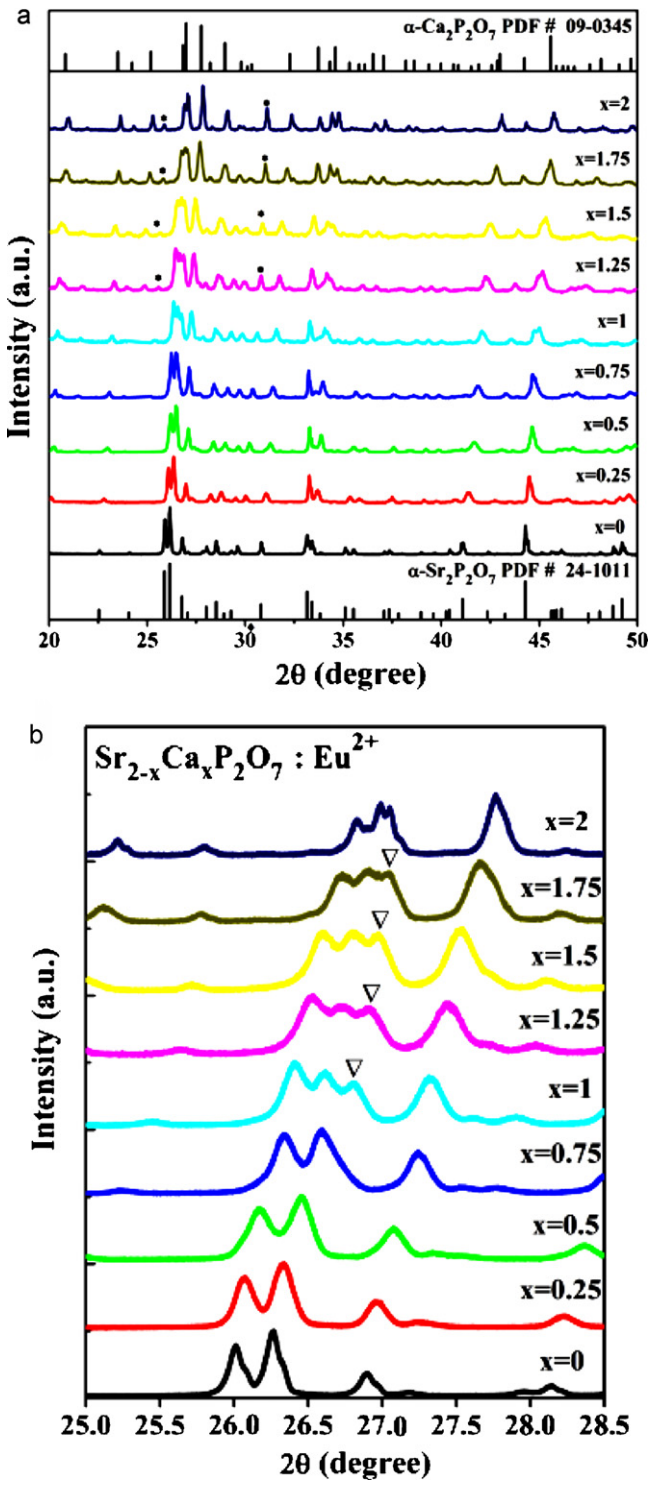

Fig. 1. (a) XRD patterns of $Sr_{2-x}Ca_xP_2O_7$:4% Eu^{2+} (x = 0, 0.25, 0.5, 0.75, 1, 1.25, 1.5, 1.75, 2) phosphors and the standard α-$Sr_2P_2O_7$ (no. 24-1011), α-$Ca_2P_2O_7$ (no. 09-0345). (*) Diffraction peak of $Ca_3(PO_4)_2$ phase. (b) Fine XRD patterns for 2θ degree within 25.0° and 28.5°.

α-$Sr_2P_2O_7$ type phase (JCPDS 24-1011) to α-$Ca_2P_2O_7$ type phase (JCPDS card 09-0345) with increasing Ca^{2+} composition x from 0 to 2. α-$Sr_2P_2O_7$ has an orthorhombic unit cell with space group *Pnma*. There are two types of Sr^{2+} sites which are both coordinated by nine oxygens [11,12]. α-$Ca_2P_2O_7$ crystallizes in the monoclinic space group $P2_1/n$. There are also two types of Ca^{2+} sites that show coordination numbers of eight [13]. In Fig. 1(a), the monotonic shift

Table 1
The lattice parameters of orthorhombic $Sr_{2-x}Ca_xP_2O_7$:Eu^{2+} ($x \leq 0.75$) with the changing of x.

x	a	b	c
0	8.39	13.046	5.468
0.25	8.822	13.005	5.391
0.5	8.804	12.978	5.347
0.75	8.775	12.969	5.353

to higher diffraction angles of the main XRD peaks with increasing x is attributed to the increasing replacement of Sr^{2+} with ionic radius of 1.12 Å by small Ca^{2+} (0.99 Å). The formation of the minor by-product $Ca_3(PO_4)_2$ phase (JCPDS 70-2065, *) is appeared for $x > 1$. The impact on our investigated photoluminescence properties can be excluded because the emission band (480 nm)[1] of $Ca_3(PO_4)_2$:Eu^{2+} is not detected in PL spectra. The fine XRD patterns for 2θ degree within 25.0° and 28.5° are exhibited in Fig. 1(b). It shows that the XRD patterns for x within 0–0.75 are identical to the α-$Sr_2P_2O_7$ type phase except of angle shift. This indicates that $Sr_{2-x}Ca_xP_2O_7$:Eu^{2+} forms a complete solid solution in α-$Sr_2P_2O_7$ type phase for $x \leq 0.75$. As $x = 1$, an additional peak (▽) appears, implying the formation of α-$Ca_2P_2O_7$ type phase, that is confirmed by the correlated luminescent properties. The lattice parameters of the orthorhombic $Sr_{2-x}Ca_xP_2O_7$:Eu^{2+} ($x \leq 0.75$) with the changing of x have been calculated out and illustrated in Table 1. As expected, the lattice parameters decrease with increasing x ascribed to the increasing replacement of Sr^{2+} with ionic radius of 1.12 Å by small Ca^{2+} (0.99 Å). For $x \geq 1$, $Sr_{2-x}Ca_xP_2O_7$:Eu^{2+} is mixed phases and the lattice parameters cannot be calculated out by a general formula.

Fig. 2(a) shows the PL (λ_{ex} = 330 nm) and PLE spectra (λ_{em} = peak positions) for $Sr_{2-x}Ca_xP_2O_7$:4% Eu^{2+} with various x. One can see both the PLE and PL spectra correlate to x. The PLE spectra cover the UV and near UV spectral region. The PL spectra strongly correlate to x, including both the positions and bandwidths, as shown in detail in Fig. 2(b). For $x = 0$, α-$Sr_2P_2O_7$:Eu^{2+} exhibits a PL band (band I) peaking at 420 nm. The band I is Gaussian type and performs a redshift from 420 nm to 435 nm with increasing x up to 1. With further increasing x, a new band (band II) appears and gradually enhances at the higher energy side of band I. The superposition of the two bands leads to a broad blue PL band that becomes the widest at $x = 1.25$. The evidence for this spectral superposition is that the distribution of the broad PL band is dependent on excitation wavelength. Fig. 3 shows the PL and PLE spectra monitored at different wavelengths for the sample with $x = 1.25$. The significant difference between the PL spectra upon 330 nm and 415 nm excitation and between the PLE spectra monitoring at 410 nm and 460 nm is remarkable, indicating different optical properties of band I and band II. Especially upon 415 nm excitation, only band I is observed, ascribing to the vanishment of the excitation of higher energy band II at this wavelength. For $x = 2$, band II is therefore originated from pure α-$Ca_2P_2O_7$:Eu^{2+}. As a result, each PL spectrum for x within 1–1.75 can be fitted by two Gaussian bands in wavenumber, in which the lower energy band is named as band I and the higher energy one is band II, as shown in Fig. 2(b).

The fitting results are literally summarized in Table 2. For band I, the peak position shifts from 420 nm to 435 nm followed by band broadening from 24 nm to 33 nm with increasing x from 0 to 1. Further increasing x beyond 1, both the position and bandwidth of band I keep unchanged. The redshift of band I is ascribed to the enhancement of the crystal field strength due to Ca^{2+} partial substitution for Sr^{2+} in α-$Sr_2P_2O_7$ type phase. The band broadening is attributed to inhomogeneous broadening due to random substitution. The inhomogeneous broadening is examined by PL spectra in the sample with $x = 0.75$, as shown in Fig. 4. Because the sample ($x = 0.75$) shows

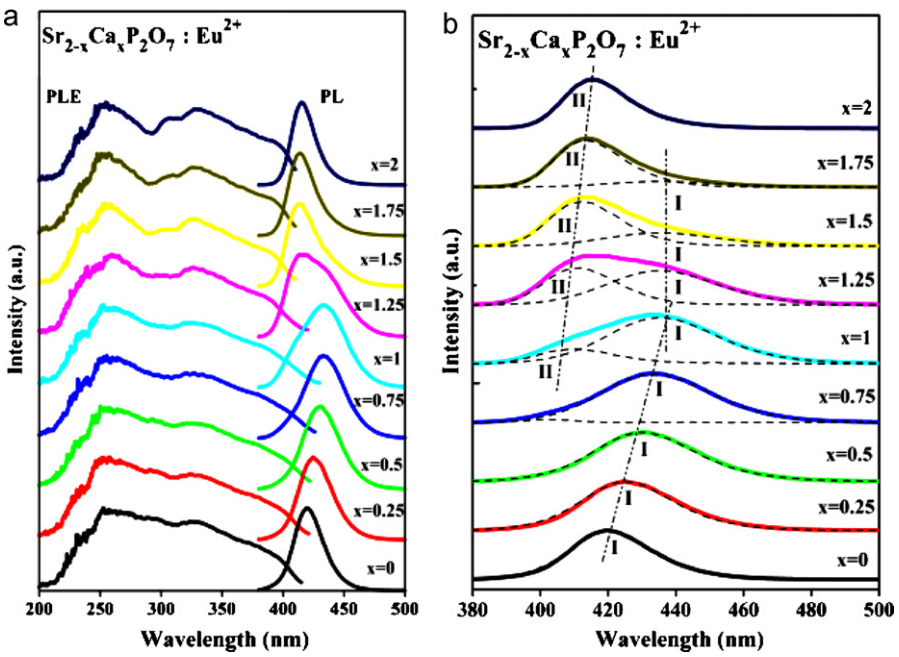

Fig. 2. (a) PL (λ_{ex} = 330 nm) and PLE spectra (λ_{em} = peak positions) for $Sr_{2-x}Ca_xP_2O_7$:4% Eu^{2+} (x = 0, 0.25, 0.5, 0.75, 1, 1.25, 1.5, 1.75, 2) phosphors. (b) PL (solid) spectra for $Sr_{2-x}Ca_xP_2O_7$:4% Eu^{2+} (x = 0, 0.25, 0.5, 0.75, 1, 1.25, 1.5, 1.75, 2) upon 330 nm excitation and the Gaussian fitting results (dash).

Table 2
Emission properties of Sr–Ca pyrophosphate compositions.

Composition	Peak position (nm) band I, band II		Width at half-height (nm) band I, band II	
α-$Sr_2P_2O_7$:4%Eu^{2+}	420		24	
$Sr_{1.75}Ca_{0.25}P_2O_7$:4%Eu^{2+}	425		27	
$Sr_{1.5}Ca_{0.5}P_2O_7$:4%Eu^{2+}	430		30	
$Sr_{1.25}Ca_{0.75}P_2O_7$:4%Eu^{2+}	434		33	
$Sr_1Ca_1P_2O_7$:4%Eu^{2+}	435	409	33	22
$Sr_{0.75}Ca_{1.25}P_2O_7$:4%Eu^{2+}	435	410	33	21
$Sr_{0.5}Ca_{1.5}P_2O_7$:4%Eu^{2+}	435	412	33	21
$Sr_{0.25}Ca_{1.75}P_2O_7$:4%Eu^{2+}	435	414	33	20
α-$Ca_2P_2O_7$:4%Eu^{2+}	416	416		20

only band I (Fig. 2), the observation of excitation wavelength dependent PL position of band I, as shown in Fig. 4, demonstrates the existence of inhomogeneous broadening. The unchanged position and width of band I for $x > 1$ is explained as follows. In view of the continuous shift of the XRD peak to higher angles, the Ca^{2+} substitution for Sr^{2+} may continuously takes place with increasing x. The observation of band II followed by appearance of the new XRD peak (▽) indicates that α-$Ca_2P_2O_7$ type phase forms for $x \geq 1$. The cease of redshift of band I for $x > 1$ is speculated to be the result of formation of deformed α-$Sr_2P_2O_7$ type phase which perhaps tends to the α-$Ca_2P_2O_7$ type phase that forces the emission band of Eu^{2+} towards the high energy side and in turn compensates the redshift of band I due to Ca^{2+} substitution for Sr^{2+}. Meanwhile, the environmental disorder of α-$Sr_2P_2O_7$ type phase reaches the maximum for $x \geq 1$.

For band II, it appears at $x = 1$ and subsequently shifts to the red side followed by band narrowing on increasing x. As a result, $Sr_{2-x}Ca_xP_2O_7$:Eu^{2+} starts to form α-$Ca_2P_2O_7$ type phase for $x \geq 1$. With increasing x, the crystal field strength is enhanced due to Ca^{2+} substitution for Sr^{2+} which therefore leads to a redshift of band II. While the environmental disorder decreases with increasing of

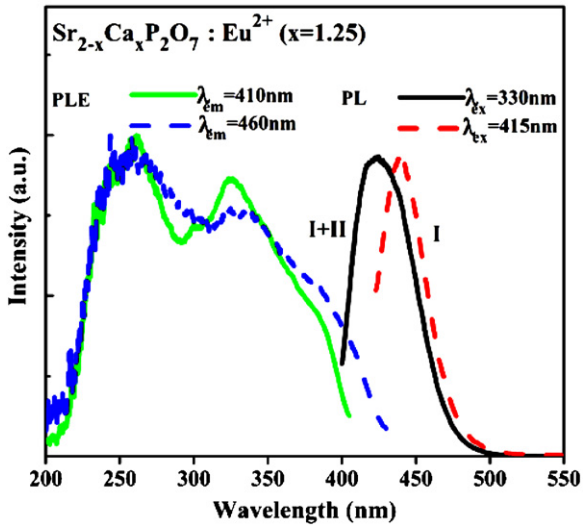

Fig. 3. PL and PLE spectra monitored at different wavelengths with x = 1.25 sample.

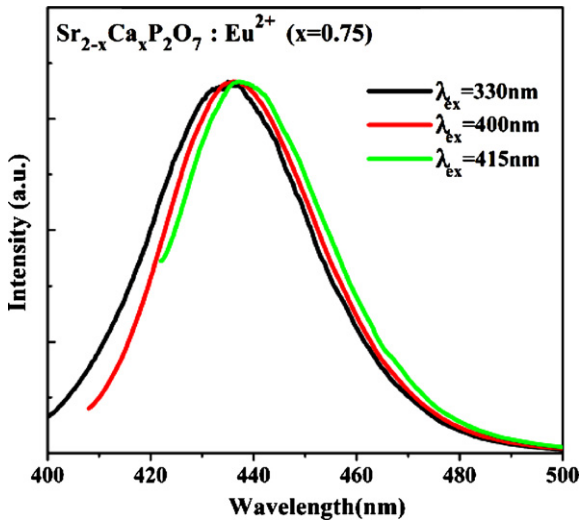

Fig. 4. PL spectra upon different excitation wavelengths with x = 0.75 sample.

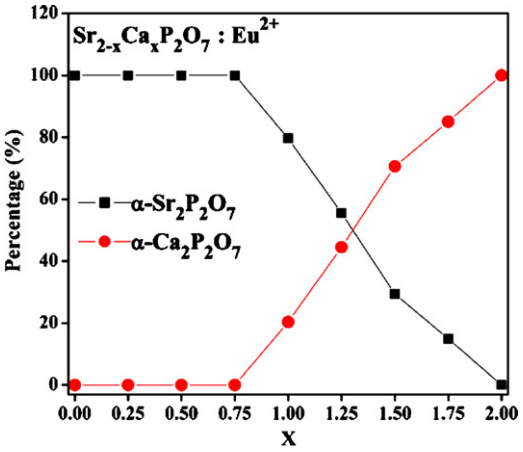

Fig. 5. The phase percentages of α-$Sr_2P_2O_7$ type phase and α-$Ca_2P_2O_7$ type phase in the phosphors.

Ca^{2+} substitution for Sr^{2+} in α-$Ca_2P_2O_7$ type phase until pure α-$Ca_2P_2O_7$ is formed for $x = 2$.

On the analysis above, the crystal phase of $Sr_{2-x}Ca_xP_2O_7$:Eu^{2+} is dependent on x. For $0 \le x \le 0.75$, the materials keep pure α-$Sr_2P_2O_7$ type phase. For $1 \le x < 2$, the systems is speculated consisting of two mixed phases of deformed α-$Sr_2P_2O_7$ type phase and pure α-$Ca_2P_2O_7$ type phase. For $x = 2$, the phosphor is pure α-$Ca_2P_2O_7$ type phase. The percentages of α-$Sr_2P_2O_7$ type phase (including pure and deformed ones) and pure α-$Ca_2P_2O_7$ type phase can be estimated based on PL spectra. We experimentally observed that the luminescence efficiency of α-$Sr_2P_2O_7$:Eu^{2+} and α-$Ca_2P_2O_7$:Eu^{2+} are almost identical under excitation in range of 250–380 nm. It is hence possible to estimate phase percentages by comparing the integrated area of band I and band II that under 330 nm excitation, as shown in Fig. 5. It demonstrates that $Sr_{2-x}Ca_xP_2O_7$:Eu^{2+} crystallizes only in α-$Sr_2P_2O_7$ type phase for x in the range of 0–0.75. For $x > 0.75$, additional phase α-$Ca_2P_2O_7$ type phase starts to form and subsequently increases with increasing x followed by percentage reduction of α-$Sr_2P_2O_7$ type phase. For $x = 2$, there exists complete α-$Ca_2P_2O_7$ type phase. The point for the equal contents of the two phases occurs at $x = 1.3$.

The fluorescence decay patterns ($\lambda_{ex} = 355$ nm) monitored at 410 nm and 460 nm (the tail of the emission band) are measured. The decay curves for $x = 0$, 1 and 2 are plotted in Fig. 6 as representatives. It is found that both decays at 410 nm and 460 nm are exponential for $x = 0$ and 2, but deviate from exponential function for x in the range of 0.25–1.75, where the decays at 410 nm become faster and that at 460 nm show a build-up component. This phenomenon reflects the characteristics of energy transfer from donors to acceptors, i.e., from high energy Eu^{2+} at 410 nm to low energy Eu^{2+} at 460 nm.

The lifetimes for fluorescence at 410 nm (τ_{410}) and 460 nm (τ_{460}) are obtained by integrating the decay curves with the normalized initial intensities. The change of the lifetimes with x is shown in Fig. 6 (bottom). It is clearly demonstrated that τ_{410} and τ_{460} vary in opposite tendency following x, reflecting the result of energy transfer which is considered to occur only within the same crystal phase. As listed in Table 2, band II is located at short wavelength and has a smaller bandwidth in comparison with band I. The energy transfer from Eu^{2+} at 410 nm to that at 460 nm is considered to occur only within band I rather than band II. For x in the range of 0–0.75, τ_{410} decreases with x. This reduction is attributed to enhanced energy transfer from Eu^{2+} at 410 nm to lower energy Eu^{2+} within the inhomogenously broadened band I of α-$Sr_2P_2O_7$ type phase. The enhanced energy transfer is resulted

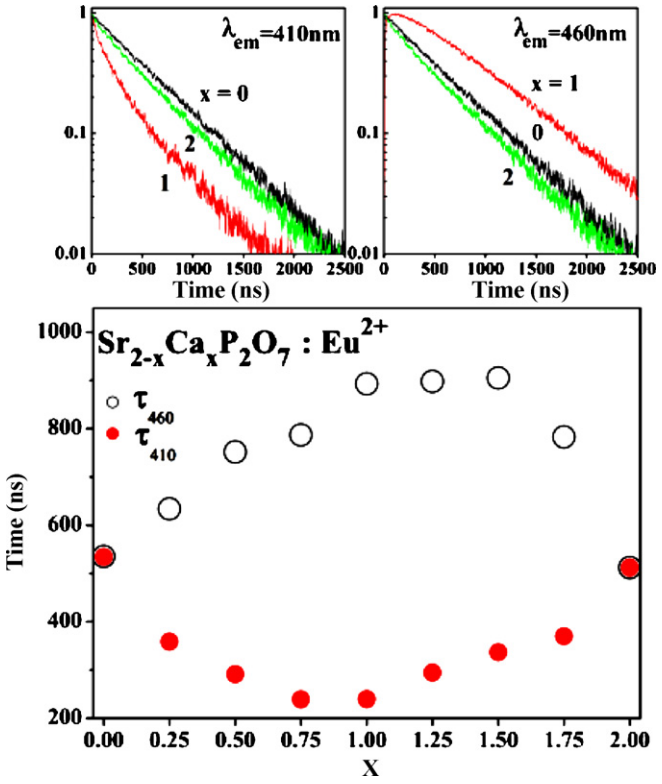

Fig. 6. Fluorescence decays monitored at 410 nm and 460 nm for $x = 0$, $x = 1$ and $x = 2$ within $Sr_{2-x}Ca_xP_2O_7$:4% Eu^{2+} ($x = 0$, 0.25, 0.5, 0.75, 1, 1.25, 1.5, 1.75, 2) phosphors. Bottom: lifetimes of 410 nm (τ_{410}) and 460 nm (τ_{460}).

from the increase of lower energy Eu^{2+} sites due to increased Ca^{2+} substitution for Sr^{2+}. For $x \ge 1$, α-$Ca_2P_2O_7$ type phase is formed followed by continues reduction of α-$Sr_2P_2O_7$ type phase. As a result, the effect of energy transfer is reduced and in turn τ_{410} gradually approaches to the fluorescence lifetime of band II in α-$Ca_2P_2O_7$. Accordingly, the increase of τ_{460} with x in the range of 0–0.75 is the result of enhanced receipt of energy for the lower energy Eu^{2+} from high energy Eu^{2+}. For $x \ge 1$, τ_{460} naturally approaches to the fluorescence lifetimes of band II in α-$Ca_2P_2O_7$ since the speculated deformed α-$Sr_2P_2O_7$ type phase vanishes for $x = 2$.

4. Conclusions

$Sr_{2-x}Ca_xP_2O_7$:Eu^{2+} ($x = 0$–2) phosphors with intense and adjustable blue emission are prepared by solid state reaction. The crystal phase of $Sr_{2-x}Ca_xP_2O_7$ is dependent on x. For $0 \le x \le 0.75$, the materials keep pure α-$Sr_2P_2O_7$ type phase. For $1 \le x < 2$, the system is speculated consisting of two mixed phases of deformed α-$Sr_2P_2O_7$ type phase and pure α-$Ca_2P_2O_7$ type phase. For $x = 2$, the phosphor is pure α-$Ca_2P_2O_7$ type phase. The percentages of α-$Sr_2P_2O_7$ type phase (including pure and deformed ones) and pure α-$Ca_2P_2O_7$ type phase can be estimated based on PL spectra. The emission band (band I) in α-$Sr_2P_2O_7$ type phase and that (band II) in α-$Ca_2P_2O_7$ type phase both shift to the red on increasing x due to enhancement of crystal field strength in case of Ca^{2+} substitution for Sr^{2+}. This substitution also leads to remarkably inhomogeneous broadening of band I, within which energy transfer from the high energy Eu^{2+} to the low energy one is observed. The superposition of band I and band II results in various distributions of intense emission band including the redshifted and more broadened ones suitable for white light generation.

Acknowledgements

This work is financially supported by the National Nature Science Foundation of China (10834006, 51172226, 10904141, 10904140), the MOST of China (2010AA03A404) and the Scientific project of Jilin Province (20090134, 20090524) and CAS Innovation Program.

References

[1] C. Costas, Lagos, J. Electrochem. Soc. 117 (1970) 1189.
[2] S. Nakamura, G. Fasol, Proc. SPIE 3002 (1997) 26.
[3] J.S. Kim, P.E. Jeon, J.C. Choi, H.L. Park, Appl. Phys. Lett. 84 (2004) 15.
[4] W.J. Yang, L.Y. Luo, T.M. Chen, et al., Chem. Mater. 17 (2005) 3883.
[5] W.J. Yang, T.M. Chen, Appl. Phys. Lett. 88 (2006) 101903.
[6] Y.Q. Li, J.E.J. van Steen, J.W.H. van Krevel, et al., J. Alloys Compd. 417 (2006) 273–279.
[7] Y.Q. Li, A.C.A. Delsing, G. de With, H.T. Hintzen, Chem. Mater. 17 (2005) 3242.
[8] Hong He, Xiufeng Song, Renli Fu, et al., J. Alloys Compd. 493 (2010) 401–405.
[9] S. Ye, Z.S. Liu, Mater. Res. Bull. 43 (2008) 1057.
[10] Z.D. Hao, J.H. Zhang, X. Zhang, X.Y. Sun, Y.S. Luo, S.Z. Lu, Appl. Phys. Lett. 90 (2007) 2611.
[11] L. Hagman, I. Jansson, C. Magneli, Acta Chem. Scand. 22 (1968) 1419.
[12] J. Barbier, J.P. Echard, Acta Crystallogr. Sect. C: Cryst. Struct. Commun. 54 (1998) IUC9800070.
[13] C. Calvo, Inorg. Chem. 7 (1968) 1345.